Nighttime Cloud Detection Over the Arctic Using AVHRR Data

D. A. Spangenberg, D. R. Doelling, and V. Chakrapani
Analytical Services & Materials, Inc.
Hampton, Virginia

P. Minnis
National Aeronautics and Space Administration
Hampton, Virginia

T. Uttal
National Oceanic and Atmospheric Administration
Boulder, Colorado

Introduction

Clouds play an important role in the Arctic energy budget. The magnitude and significance of the radiative impact of polar clouds, however, are not well known. Polar nocturnal clouds are often warmer or at the same temperature as the background snow surface, complicating cloud detection. Also, these clouds tend to be thin, with lower emittances than clouds occurring during the summer. Using only the infrared (IR) channels of satellite data to characterize cloud amount and distribution in the Arctic is difficult, especially determining cloud amounts visually from the surface in the dark. However, the cloud data taken from surface instruments during the Surface Heat Budget of the Arctic Ocean (SHEBA) field experiment can serve to validate and improve satellite cloud detection.

The National Oceanic and Atmospheric Administration (NOAA) advanced very high-resolution radiometer (AVHRR) channel-3 (T3; 3.7µm), channel-4 (T4; 11µm), and channel-5 (T5; 12µm) brightness temperature bands are used to derive nighttime cloud amounts over SHEBA. The cloud amounts are based on a brightness temperature threshold approach. Satellite-derived cloud amounts from the nighttime cloud algorithm are validated by comparing them to NOAA Environmental Technology Laboratory (ETL) millimeter-wave cloud radar (MMCR), NOAA ETL depolarization aerosol and backscatter unattended lidar (DABUL), and surface observer cloud amounts over the SHEBA site. Broadband longwave (LW) fluxes are computed from narrowband satellite data using the empirical technique of Doelling et al. (2001). Cloud forcing at the top of the atmosphere (TOA) is then computed over the Arctic Ocean in the SHEBA vicinity.

Satellite Data

For this study, all NOAA-12 and -14 AVHRR-high-resolution picture transmission (HRPT) satellite orbits that encompass the SHEBA site are used to develop a January-through-March 1998 dataset of

1,010 images. All hours are sampled by NOAA-12 and -14 except for 6-10 Universal Time Coordinates (UTC). The cloud mask algorithm was applied at the 1-km pixel level and the resulting clear-sky and cloudy products were averaged within a 25-km radius around the SHEBA site and within 56×56-km2 regional grid boxes. Figure 1 shows the SHEBA ship track and boundary of the regional grid. Satellite cloud amounts in this study are defined as the ratio of the cloudy pixels to the total number of pixels.
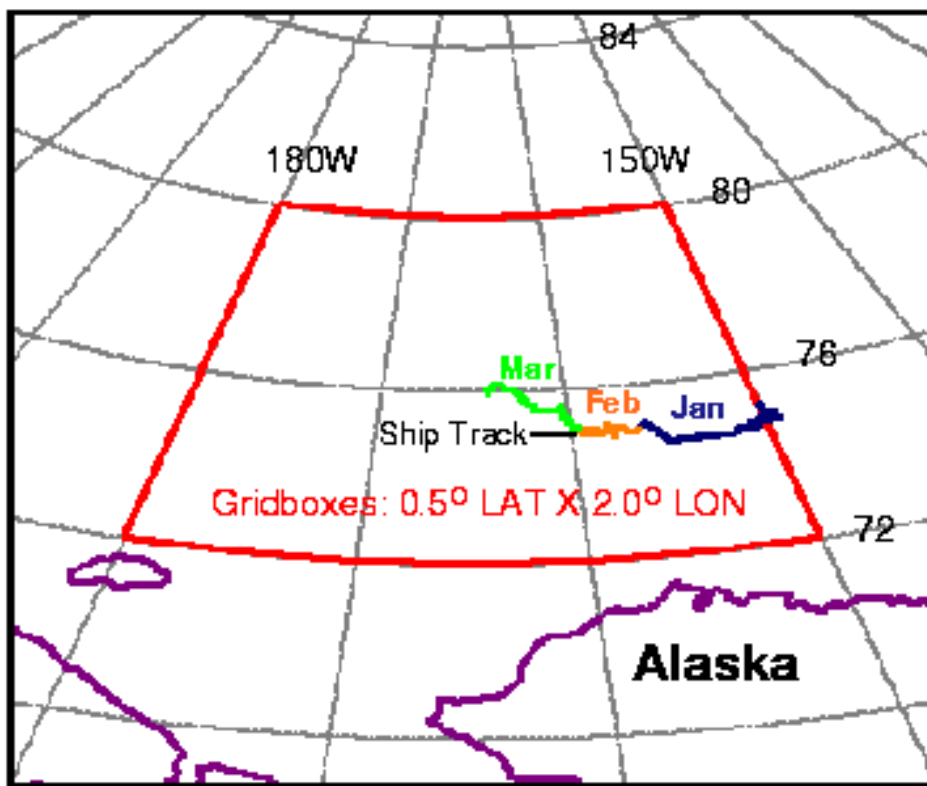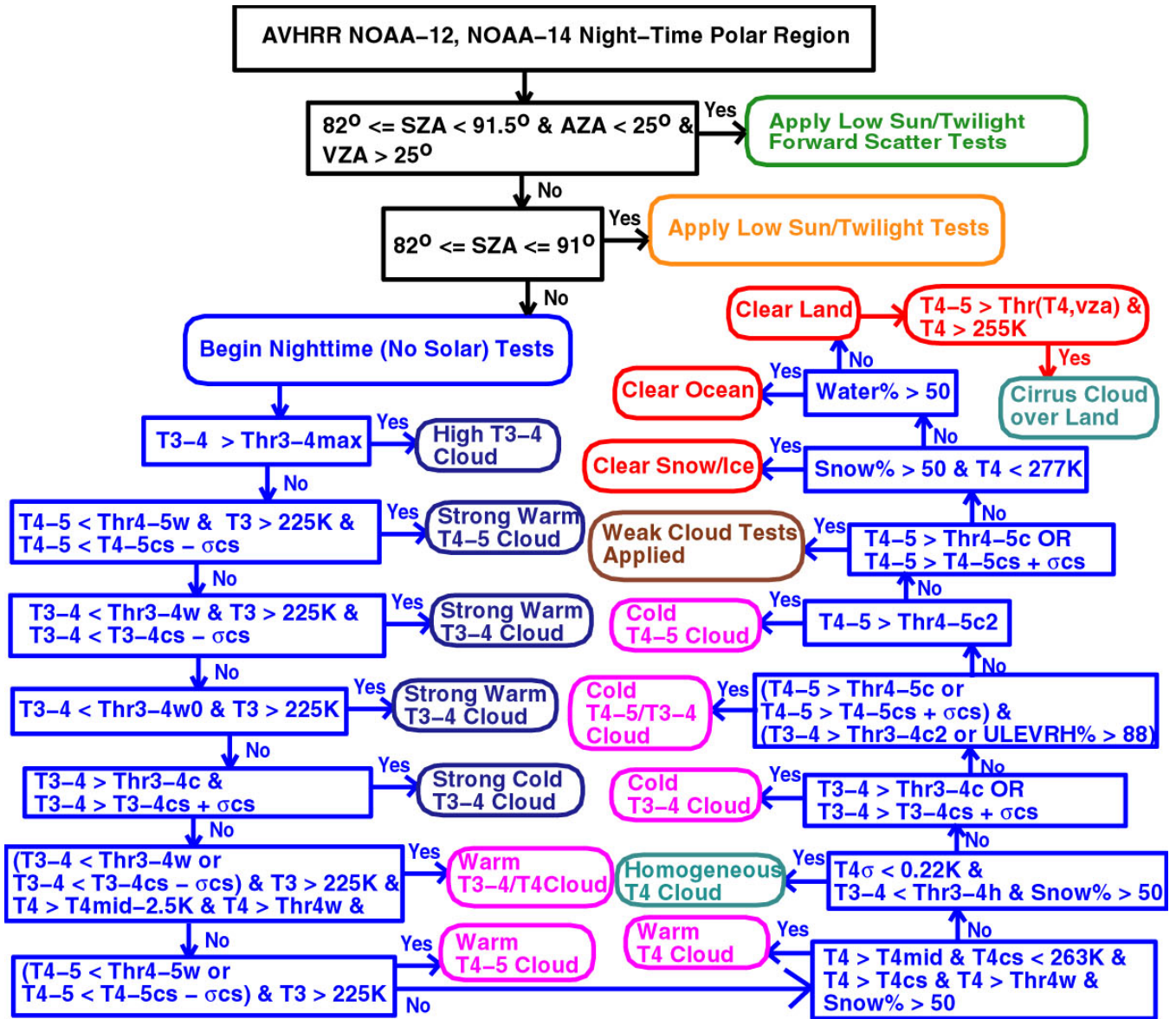

Figure 1. SHEBA ship track and analysis domain.

Technique

To remove noise inherent in the 3.7-µm band at low temperatures, the images were filtered using a parametric Wiener filter developed by Simpson and Yhann (1994). This method works well at night when the T3 and T4 images are similar. Because some noise can still be left in the T3-4 images, they were smoothed using averages of 16×16 pixels.

Fixed image-independent thresholds were used to derive the satellite cloud mask. The thresholds include T3-4, T4-5, T4, the median T4 for the image (T4mid), and the T4 spatial standard deviation (T4σ). Because of the calibration differences between NOAA-12 and -14, a different set of thresholds was used for each satellite. The Clouds and the Earth's Radiant Energy System (CERES) nocturnal polar cloud mask framework (Trepte et al. 2001) was modified to work with the NOAA-AVHRR channels. Figure 2 shows the flowchart of the polar cloud mask algorithm for AVHRR. The algorithm

Figure 2. Flowchart of the polar nighttime cloud mask for AVHRR.

is applied when the solar zenith angle (SZA) is greater than 82°. Clear-sky a priori temperature values at the TOA were computed using a correlated k-distribution method (Kratz 1995) incorporating the European Centre for Medium-Range Weather Forecasts (ECMWF) profiles. The polar mask first performs a series of cloud tests shown in Figure 2. If any of the 12 cloud tests pass, the pixel is considered to be cloudy. If the tests fail, then the pixel's T4-5 value is checked. If that value is below a certain threshold, the pixel is classified as clear sky and is subdivided into snow, ocean, or land. Because the remaining pixels are difficult to classify during the polar night, weak clear and weak cloud categories were defined. For a pixel to be classified as weak clear or weak cloud, the T4-5 value had to be above 0.5K for NOAA-12 or 0.3K for NOAA-14. The weak categories often contain surface-based aerosol haze, thin cirrus, thin fog, steam fog, or diamond dust. Since the cloudy T4 and T3-4 pixels are similar to the underlying surface in the weak categories, thresholding is not always reliable. Consequently, the weak categories should be used with caution since confidence in cloud detection is fairly low for these cases.

Note that different tests must be used to pick out warm versus cold clouds in the flowchart (Figure 2). The NOAA-12 warm cloud T3-4 tests, which detect a majority of the clouds, require T3-4 to be below -1.5K for strong clouds, -0.6K for most clouds, and -0.3K for weak clouds. The corresponding NOAA-14 thresholds are 0.7K, 1.9K, and 2.2K, respectively. For warm clouds, T4 must exceed 239K. Threshold detection for cold clouds is used if T3-4 is greater than 1.4K for NOAA-12 and 4.0K for NOAA-14. For twilight conditions (82° < SZA < 91°), the cloud mask was modified to account for the weak visible signature in the T3 image. This was done by increasing the T3-4 thresholds and by adding an additional cloud test for relatively high T3-4 values in warm clouds. A special case of twilight tests is applied for forward scatter at high satellite view angles. This is necessary because of the very high reflectance of T3-4 for this viewing geometry. An example of the cloud mask output, along with NOAA-14 T3-4, T4, and T4-5 images for 15:14 UTC, 11 January 1998, are shown in Figure 3. The SHEBA site is located in an area of thin warm fog, in the dark region near the center of the T3-4 image. The area of high T4 and T3-4 values in the right-hand part of the imagery represents a warm cloud system. The clear area in the upper (northern) part of the T3-4 and T4 imagery has values that are nearly the same as the cirrus in the lower-right (southern) part of the images. This example illustrates the difficulty of detecting cirrus during the polar winter night.

Results

Satellite Validation

The satellite-derived cloud amounts were validated by comparing them with NOAA ETL cloud radar amounts over SHEBA for the months of January through March 1998. The DABUL system was used to detect thin, low-lying fog or thin cirrus clouds that are not always observed in the MMCR (Intrieri et al. 2002). DABUL data were only available for January and March 1998. SHEBA 6-hourly surface observer cloud amounts were also compared to the cloud radar and were used as a basis for the satellite and radar comparisons. The satellite cloud amounts were computed for a 25-km radius around the SHEBA ship. Radar cloud amounts are 20-minute time averages of processed 10-second cloud boundary data centered at the satellite times. Lidar cloud amounts are the averages of the two 10-minute intervals of processed cloud layer data centered at the satellite times.
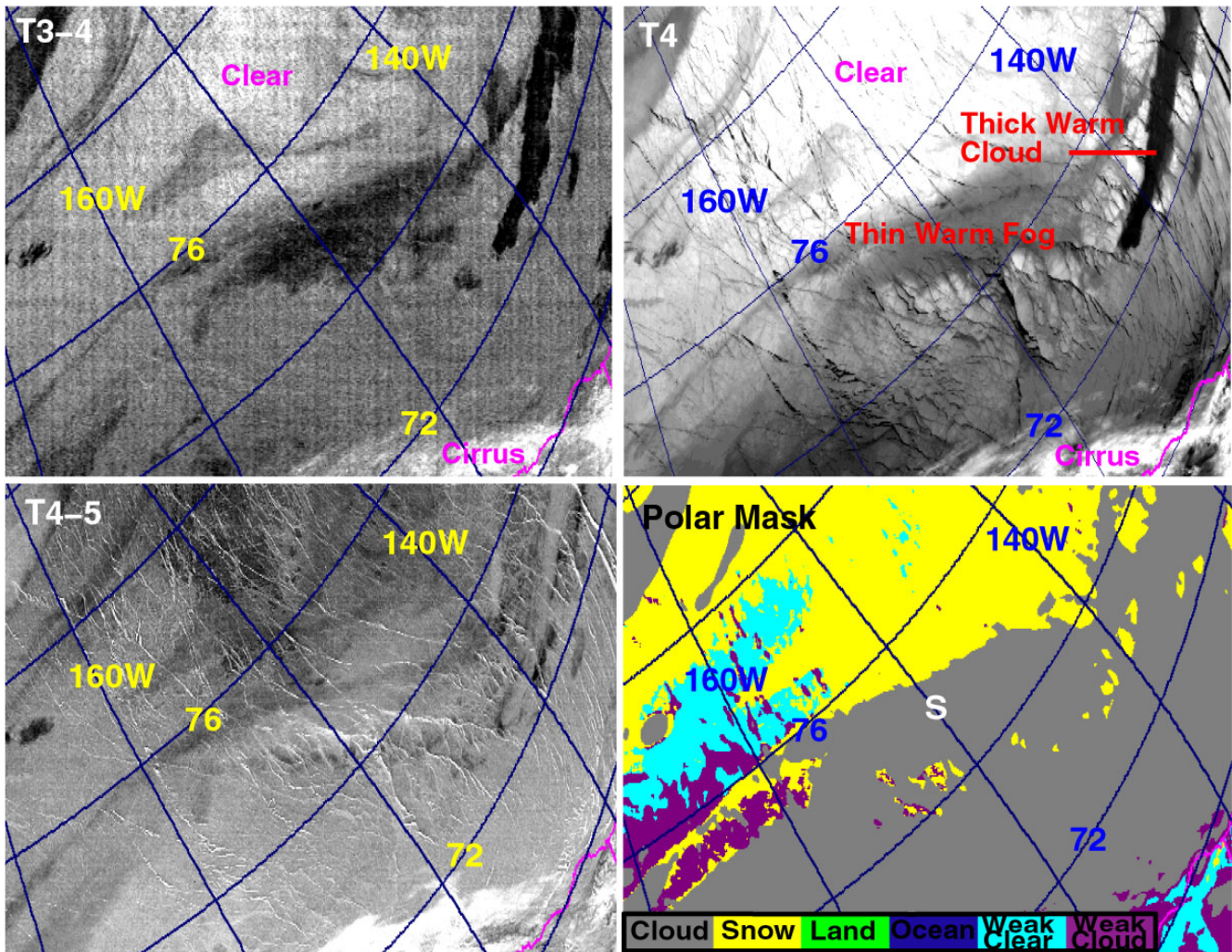
Figure 3. NOAA-14 satellite image valid at January 11, 1998, 15:14 UTC showing mixed clouds. The SHEBA location is denoted by the "S" in the polar mask.

Monthly statistics of satellite and radar cloud coverage, including means and root-mean-square (rms) errors, are shown in Table 1. The statistics were broken down into three radar reflectance (ref) categories representing strong cloud signals (ref >= -20 dBZ), weak signals (-50 dBZ < ref < -20 dBZ), and clear sky (ref <= -0 dBZ). The "All" category in Table 1 represents all radar reflectance categories combined. DABUL was used to confirm that the clear radar category was actually clear. If the lidar detected a cloud, while the radar indicated clear sky, that particular radar measurement was excluded from the statistics. Weak categories in the polar cloud mask exceeding 10% were not used in the validation. Also, for March 1998, six clear cases were not used because they are suspected to contain thin ground fog. For the 3 months, most of the rms error between the satellite and radar cloud amounts occurs for reflectances between -20 and -50 dBZ. This is the low reflectance category where some of the clouds are beyond the threshold limits of detection by the satellite at night. There is very little or no difference in T3-4 between the clouds and snow surface for this radar category; the emissivities of these types of clouds and the surface are nearly the same. Strong cloud signals in the radar, indicated by

Table 1. SHEBA ship monthly cloud amount statistics for the radar and satellite. (a) January, (b) February, and (c) March 1998 period.

(a)

Radar Reflectance (dbz)	Radar%	Sat[+]%	RMS%	#Radii
ref >= -20	100	94.3	17.2	66
-50 < ref < -20	85.9	74.4	44.7	44
ref <= -50	30.6 (0.0)	10.6	38.3 (24.7)	89
All	65.9 (52.3)	52.5	34.4 (28.3)	199

( ) - Radar cloud% set to 0.0 for ref <= -50 dBZ.
+   - Radii with weak cloud mask categories greater than 10% were not used.

(b)

Radar Reflectance (dbz)	Radar%	Sat[+]%	RMS%	#Radii
ref >= -20	100	99.0	3.7	49
-50 < ref < -20	94.3	40.0	72.2	40
ref <= -50	13.2 (0.0)	1.3	22.3 (5.6)	59
All	63.9 (58.6)	44.1	39.8 (37.4)	148

(c)

Radar Reflectance (dbz)	Radar%	Sat[+]%	RMS%	#Radii
ref >= -20	99.3	95.7	17.1	72
-50 < ref < -20	92.7	84.6	32.3	44
All	93.5 (92.0)	89.8	26.5 (27.3)	122

reflectances at or above -20 dBZ, are usually captured by the satellite very well. The February data in this reflectance category had the best agreement with the satellite cloud amounts, which were within 1% of the radar cloud amount and had an rms error of only 3.7%. During other months, the rms errors in the high reflectance category are about 17%. If it is assumed that the sky is essentially clear for radar reflectivities less than or equal to -50 dBZ (radar clutter), the statistics generally improve for all 3 months. This is indicated by the blue numbers in parentheses in Table 1 for the last two-reflectance categories. A significant rms error may arise for the clear radar (and lidar) cases. In those instances, the satellite may see some obscuration that is too thin, low, or diffuse to be clearly seen by the ground-based measurements or that may not pass directly over the ship. When all three radar reflectance categories are combined, the satellite and clutter-free radar (blue numbers in Table 1) monthly mean cloud amounts differ by only 0.2%, 14.5%, and 2.2% for January, February, and March, respectively.

The corresponding statistics between the observer and radar cloud amounts are shown in Table 2. For strong radar cloud signals, rms errors are much higher than the satellite errors, indicating the observer is missing some strong radar cloud signals. Weak cloud radar signals are more frequently missed, with rms errors similar to the satellite errors. It is difficult for a surface observer to determine nighttime cloud coverage accurately by looking at star visibility. Stars may be visible even through thin clouds, leading to an underestimation of cloud at night. Schneider et al. (1989) have shown that observers greatly underestimate thin and scattered cloud cover when the sky is dark with little or no moonlight.

Table 2.   SHEBA ship cloud amount statistics for the cloud radar and surface observer. (a) January, (b) February, and (c) March 1998 period.

(a)

Radar Reflectance (dbz)	Radar%	Obs%	RMS%	#Obs
ref >= -20	100	86.8	34.1	36
-50 < ref < -20	95.2	43.3	69.3	15
ref <= -50	34.9 (0.0)	9.1	38.7 (16.4)	48
All	67.7 (50.7)	42.6	42.7 (35.1)	99

( ) - Radar cloud% set to 0.0 for ref <= -50 dBZ.

(b)

Radar Reflectance (dbz)	Radar%	Obs%	RMS%	#Obs
ref >= -20	100	88.3	24.5	33
-50 < ref < -20	95.0	46.9	62.9	16
ref <= -50	23.4 (0.0)	13.2	38.4 (25.1)	51
All	60.1 (48.2)	43.4	49.2 (33.4)	100

(c)

Radar Reflectance (dbz)	Radar%	Obs%	RMS%	#Obs
ref >= -20	100	87.9	29.8	31
-50 < ref < -20	96.2	53.5	58.6	18
ref <= -50	33.3 (0.0)	11.1	45.8 (14.0)	9
All	88.5 (88.3)	65.3	42.2 (39.0)	58

Also, over the Arctic Ocean, there is no sky glow from surface-based lighting to illuminate the bottoms of the clouds. Thus, it is hard to identify thin low clouds or fogs that may be present. Compared to the cloud radar, the surface Observers reported 8.1%, 4.8%, and 23% too few clouds for January, February, and March, respectively. Overall, the satellite rms errors are mostly less than the observer errors in all reflectance categories, indicating the satellite cloud mask technique provides a better estimate of cloud amount than the visual observations.

SHEBA Domain Results

Monthly averaged cloud amounts and T4 values were derived for January through March 1998 using the time and space averaging methods of Young et al. (1998). The values were computed over the regional domain grid encompassing the SHEBA site (Figure 1). Fewer images for March were used since daylight images were excluded from the analysis. The cloud amount, clear T4, and cloudy T4 maps are shown in Figure 4. The cloud amounts are higher over the southern part of the domain for all three months, with values between 50% and 80%. The SHEBA ship was located in an area with 45% cloud coverage during January and February, with values increasing to 75% in March. Most notable is the dramatic increase of clouds from February to March, probably associated with the changing seasons. For all 3 months, the cloudy temperatures are noticeably higher than the clear-sky temperatures,
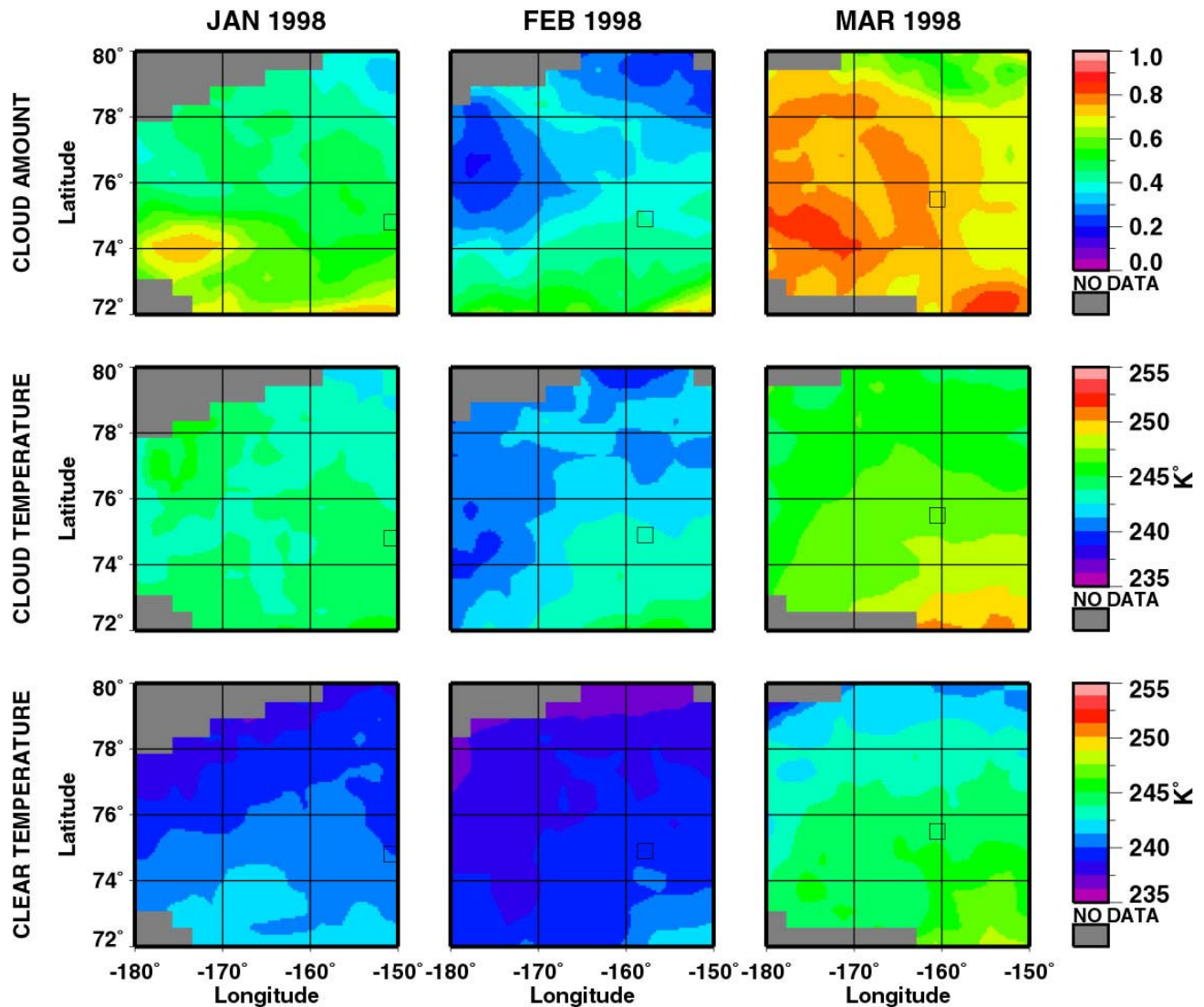
Figure 4. SHEBA domain cloud amounts and temperatures on the regional grid for January-March 1998.

indicating that warm clouds are most common during the long winter night over the Arctic Ocean. February had the lowest clear-sky temperatures, with typical values around 238K. Table 3 shows a comparison between monthly mean cloud, weak cloud, and weak clear amounts for January through March 1998. Both clear-sky and cloud temperatures are shown. The total cloud percentage column shows the cloud cover for all cloud categories combined. Nighttime cloud cover over the western Arctic Ocean is at a minimum of 37% during February and at a maximum of 72% in March. In all 3 months, the sum of the weak amounts ranges from 24% to 34% with the weak clear exceeding the weak cloud areas. Because of the relatively high amount of weak clear ranging from 14% to 25 %, it is likely that the total cloud amounts should be somewhat higher due to cloud contamination within the weak clear category. The blue numerals in Table 3 under the weak categories are for percentages relative to the total cloud or clear amounts. These numbers show the relative dominance of the weak categories in the

polar mask. Weak clouds account for as much as 24% of all clouds during February. Weak clear ranges up to 50% of all clear areas in March. The mean cloud temperature followed the same trend as the clear-sky background with the mean cloud temperature exceeding the clear-sky values by 3-4K for all three months.

Table 3. SHEBA domain cloud statistics from the polar cloud mask for January-March 1998. Blue numbers in parenthesis are for percent of the total cloud or clear amounts.

Month	# Images	Total Cloud%	Weak Cloud%	Weak Clear%	T4 Clear (K)	T4 Cloud (K)
Jan	350	50.8	10.1 (19.9)	13.7 (27.8)	240.0	243.9
Feb	312	36.5	8.9 (24.4)	24.6 (38.7)	238.8	241.7
Mar	285	72.1	11.0 (15.3)	14.0 (50.2)	243.8	246.5

For the broadband flux results, the AVHRR narrowband IR fluxes were converted into broadband LW fluxes using the method outlined in Doelling et al. (2001). Figure 5 shows the winter and spring regression fits used to obtain the January-through-March 1998 broadband LW fluxes. Earth Radiation Budget Experiment (ERBE) and NOAA-9 AVHRR data from 1986 were matched to obtain the regression fits. The different lines are for constant values of column-weighted relative humidity (RH) above the radiating surface. The broadband LW flux M_{lw} is computed from the equation

$$M_{lw} = a0 + a1*M_{ir} - a2*M_{ir}^2 - a3*Mir*\ln(RH),$$

where M_{ir} is the narrowband IR flux and a0, a1, a2, and a3 are the coefficients of the regression fit. M_{lw} was computed using both the winter and spring regression fits, with the resulting values time interpolated to the appropriate month of 1998. LW cloud forcing is defined as

$$LWCRF = M_{lwclr} - M_{lw},$$

where M_{lwclr} is the clear-sky LW flux and M_{lw} is the total-sky LW flux. Typical outgoing LW flux values range from 165-180W/m^2 in clear-sky regions, with slightly more energy being lost for the total-sky case. This leads to a net loss of energy of about 2-6 W/m^2 at TOA due to clouds (negative LWCRF). Although wintertime Arctic clouds are primarily warmer than the surface and increase the underlying surface temperature, the overall effect on the earth-atmosphere system is a loss of energy at TOA. Domain averages of TOA LWCRF, along with the LW fluxes, are shown in Table 4. February 1998, the month with minimum cloudiness, has the weakest cloud-forcing signal of -2.4 W/m^2. March 1998 has the most pronounced loss of energy at TOA, -4.1 W/m^2. This corresponds to the month of maximum cloudiness.

Table 4. SHEBA domain broadband LW flux statistics for January-March 1998.

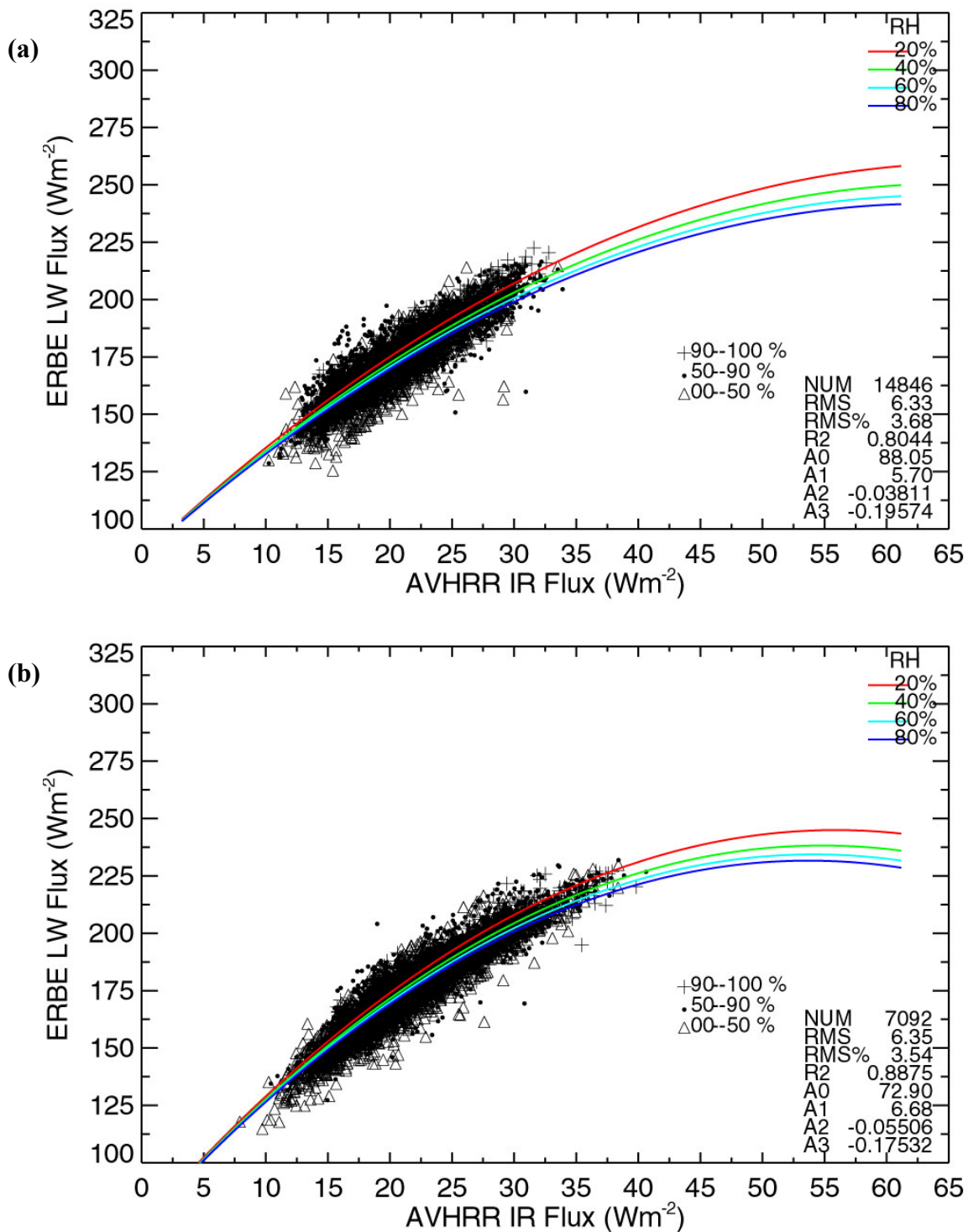| Month	Clear LWF (W/m^2)	Total LWF (W/m^2)	LWCRF (W/m^2)
Jan	170.1	174.0	-3.9
Feb	167.6	170.0	-2.4
Mar	175.4	179.5	-4.1

(a)

(b)

Figure 5. Regression fit over the Arctic between AVHRR NOAA-9 narrowband IR flux and ERBE broadband LW flux data. (a) November-January 1986 and (b) February-April 1986 period.

SHEBA Ship Results

To determine how frequently clouds were actually detected in the MMCR data within the weak clear and weak cloud categories, the radar cloud amounts were compared to their satellite counterparts when the satellite cloud mask yielded large amounts of the weak cloud or weak clear category at the SHEBA site. For 18 cases when the polar mask had weak cloud amounts greater than 85%, the MMCR mean cloud amount was 72.2%. For 78 cases when the polar mask's weak clear category was above 85%, the radar reported clear skies 61.3% of the time. Further attempts to adjust the thresholds failed to close the gap between the satellite polar mask and the ground-based data. In both the weak clear and weak cloud areas, T4-5 values are high. This is a signature of relatively high moisture content, which mainly occurred in the boundary layer for this study. High moisture content, coupled with strong temperature inversions, will help support the formation and maintenance of diamond dust, diffuse ground fog, or haze. These phenomena can be invisible to the radar and lidar, but detected as weak cloud in the satellite polar mask. Much of the discrepancy between the weak clear amount from the polar mask and the ground-based clear-sky amount arises where the radar reflectance is less than -10 dBZ and very little signature of the cloud exists in the imagery. Typically, this is the case for thin or scattered cirrus. Also, some mixed cloud scenes where cirrus overlays a warm cloud below can be missed as weak cloud in the polar mask.

The monthly mean values of the satellite cloud amount, T4, LW flux, and LWCRF were computed for the area within a 25-km radius surrounding the SHEBA ship. For March 1998, 35% of the images were not used because they were taken during the daytime. Table 5 shows that cloud coverage is at a minimum of 39% in February, with values up to 77% in March. This is the same trend observed in the cloud coverage over the regional grid. The clear-sky temperatures are consistently lower than the cloud temperatures by 3-4K, leading to a negative cloud forcing of -3 to -4 W/m^2. These values are similar to the regional grid averages, suggesting the SHEBA ship was in an area representative of the rest of the western Arctic Ocean. The weak categories have a smaller temperature difference than their counterparts, leading to a dampened LW cloud forcing if only the weak clear and weak cloud areas are considered.

Table 5. SHEBA ship cloud amount, cloud temperature, and cloud forcing statistics from the polar cloud mask for January-March 1998.

Month	# Images	Cloud%	T4 Clear (K)	T4 Cloud (K)	Clear LWF (W/m^2)	Total LWF (W/m^2)	LWCRF (W/m^2)
Jan	327	46.8	240.2	244.3	170.8	174.1	-3.4
Feb	292	38.9	239.2	242.9	168.7	172.1	-3.4
Mar	211	77.0	244.8	247.1	177.3	181.3	-4.0

Summary and Future Work

An automated NOAA-AVHRR cloud detection algorithm was developed for polar regions during the nighttime. Cloud thresholds used in this study were developed using January-March 1998 satellite data over the Arctic Ocean surrounding the SHEBA ship. However, they should be applicable to other months or regions of the Arctic with minimal or no adjustment. The satellite-derived cloud amounts

agreed well with radar cloud amounts at the SHEBA site for either high radar reflectances or clear-sky radar times. The rms errors between the satellite polar cloud mask and cloud radar results were between 4% and 25% for these cases. The rms errors for low-reflectivity radar clouds were much higher, both for the satellite and surface observer. Since the cloud lidar failed to capture all of the radar returns with reflectances less than -20 dBZ, some of the error is likely due to radar clutter. Overall, the polar mask performed much better than the surface observers, who usually underestimated nighttime cloud coverage. Over the Arctic in winter, the clouds are primarily warmer than the cold background snow surface. The coverage increased from 37% in February to 72% in March 1998. The clouds acted to cool the earth-atmosphere system with a 2 to 4 W/m^2 loss of energy at the TOA.

The cloud mask algorithm will be applied to NOAA-AVHRR data taken over the Atmospheric Radiation Measurement (ARM) Program - North Slope of Alaska site during 2000 and 2001. The CERES polar cloud mask will be applied to the corresponding TERRA-MODIS data. Additional satellite-derived cloud products, including estimates of optical depth and cloud height will be available for both day and night overpasses. Cloud and radiation products can be found on the web page, http://www-pm.larc.nasa.gov.

Corresponding Author

Douglas Spangenberg, d.a.spangenberg@larc.nasa.gov, (757) 827-4647

Acknowledgments

References

Doelling, D. R., P. Minnis, D. A. Spangenberg, V. Chakrapani, A. Mahesh, F. P. J. Valero, and S. Pope, 2001: Cloud radiative forcing at the top of the atmosphere during FIRE ACE derived from AVHRR data. *J. Geophys. Res.*, **106**, 15,279-15,296.

Intrieri, J. M., M. D. Shupe, T. Uttal, and B. J. McCarty, 2002: An annual cycle of Arctic cloud characteristics observed by radar and lidar at SHEBA. *J. Geophys. Res.*, in press.

Kratz, D. P., 1995: The correlated-k distribution technique as applied to the AVHRR channels. *J. Quant. Spectrosc. Radiative Transfer*, **53**, 501-517.

Schneider, G., P. Paluzzi, and J. Oliver, 1989: Systematic error in the synoptic sky cover record of the South Pole. *J. of Climate*, **2**, 295-302.

Simpson, J. J., and S. R. Yhann, 1994: Reduction of noise in AVHRR channel-3 data with minimum distortion. *IEEE Trans. Geosci. and Remote Sens.*, **32**, 315-328.

Trepte, Q., R. F. Arduini, Y. Chen, S. Sun-Mack, P. Minnis, D. A. Spangenberg, and D. R. Doelling, 2001: Development of a daytime polar cloud mask using theoretical models of near-infrared bi-directional reflectance for ARM and CERES. *Proc. AMS 6th Conf. on Polar Meteorology and Oceanography,* May 14-18, 2001, 242-245, San Diego, California.

Young, D. F., P. Minnis, G. G. Gibson, D. R. Doelling, and T. Wong, 1998: Temporal interpolation methods for the Clouds and the Earth's Radiant Energy System (CERES) Experiment. *J. Appl. Meteorol*., **37**, 572-590.